Solubility of Cortisone and Hydrocortisone in Supercritical Carbon Dioxide and Ethanol

Journal of Chemical&Engineering Data

pubs.acs.org/jced

Article

# Solubility of Cortisone and Hydrocortisone in Supercritical Carbon Dioxide and Ethanol

Luigi Manna and Mauro Banchero*

Cite This: *J. Chem. Eng. Data* 2023, 68, 601−611

Read Online

ACCESS | Metrics & More | Article Recommendations | Supporting Information



**ABSTRACT:** Cortisone and hydrocortisone are poorly water-soluble corticosteroids widely used to treat many inflammatory and immune diseases. In the prospect of employing them in pharmaceutical applications or analytical techniques involving cosolvent-modified supercritical fluids, their solubility has been determined, for the first time, in a mixture of supercritical $CO_2$ and 2, 3, or 4 mol % of ethanol, at 318.15, 328.15, 348.15, and 373.15 K, and in the pressure range of 13−27 MPa. Tests were conducted in a semi-flow laboratory apparatus, and results were fitted with the most popular density-based correlations reported in the literature for ternary systems. Even though the two drugs exhibit similar molecular structures, the solubility of cortisone in the ethanol-sc$CO_2$ mixtures is on average 3.5 times higher than that of hydrocortisone. This is congruent with the fact that the solubility of cortisone in pure ethanol is higher. The seven-parameter Reddy−Madras model (adjusted absolute average percent deviation (AARD%) = 8.8%) proved to be the best correlating one for cortisone while the six-parameter Garlapati−Madras approach (AARD% = 11.6%) provided the best fitting for hydrocortisone. The reliability of the experimental results was also confirmed by the positive response to the Méndez-Santiago−Teja self-consistency test.

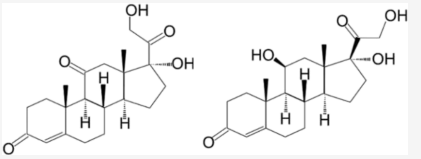

## 1. INTRODUCTION

Supercritical carbon dioxide (sc$CO_2$) is a benign solvent that has been widely employed in many pharmaceutical applications, such as drug delivery, tissue engineering, bio-imaging, and other biomedical applications.[1] In particular, it can be used to process poorly water-soluble drugs whose limited solubility in aqueous media strongly affects the dissolution rate and bioavailability in pharmaceutics.[2]

Dissolution rate enhancement of this class of drugs can be achieved by means of various solvent/antisolvent supercritical micronization techniques,[1,2] such as rapid expansion of supercritical solutions (RESS), gas antisolvent (GAS), and supercritical antisolvent (SAS). Particle size reduction, in fact, is a significant tool to achieve a higher dissolution rate of poorly water-soluble drugs in aqueous media since it increases the saturation solubility and the specific surface area of the solute.[2,3] When the solvent power of sc$CO_2$ versus the drug is exploited, drug micronization can be obtained by dissolving it in the supercritical solvent and achieving its precipitation into fine particles by expanding the compressed fluid through a nozzle (RESS process).[1] Otherwise, the drug is dissolved in an organic solvent, which is then mixed with sc$CO_2$; during the process, the mixture expands to supersaturation, and sc$CO_2$ acts as an antisolvent, causing the precipitation of the solute particles (GAS and SAS processes).[1]

The supercritical solvent impregnation (SSI) of polymeric carriers or porous matrices is another technique to prepare drug delivery vehicles for poorly water-soluble drugs.[1,4] This technique mainly aims at converting the highly crystalline structure of the drug, which hinders its dissolution in water, into a readily soluble amorphous one. It consists in dissolving the drug in the supercritical solvent in the presence of a solid carrier. Upon depressurization, if the molecular interactions between the drug and the carrier are favorable, this can result in the drug being precipitated and dispersed in its amorphous form in the solid, which results in a huge increase of its aqueous dissolution rate.[1,4]

The benefit of employing supercritical fluid technologies in pharmaceutics lies in several advantages such as the mild critical point of $CO_2$ (74 bar and 31 °C), which allows thermolabile compounds to be processed, or the tunable solvent power of sc$CO_2$, which allows solid dispersions or pharmaceutical particles with different physical states, morphologies, and size distributions to be obtained.[4,5] Sc$CO_2$ also offers the possibility to conduct the manufacturing process in an oxygen-free protective atmosphere[4] while solvent-free pharmaceutical products can be eventually obtained through a simple depressurization step.[6] Furthermore, sc$CO_2$ can also be used in analytical techniques such as supercritical fluid chromatography (SFC). In fact, the pharmaceutical interest in SFC has recently been renewed thanks to the introduction of new instruments and columns able to overcome the limitations of this technique, such as poor UV sensitivity, weak quantitative performance, and limited

**Received:** November 7, 2022
**Accepted:** January 24, 2023
**Published:** February 2, 2023

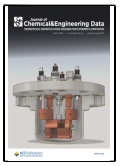

Table 1. IUPAC Name, CAS Number, Structure, and Melting Range[a] of the Drugs

| | IUPAC name | CAS | structure | melting range (°C) |
|---|---|---|---|---|
| cortisone | (8S,9S,10R,13S,14S,17R)-17-hydroxy-17-(2-hydroxyacetyl)-10,13-dimethyl-1,2,6,7,8,9,12,14,15,16-decahydrocyclopenta[a]phenanthrene-3,11-dione | 53-06-5 | 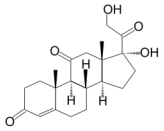 | 223-228 |
| hydrocortisone | (8S,9S,10R,11S,13S,14S,17R)-11,17-dihydroxy-17-(2-hydroxyacetyl)-10,13-dimethyl-2,6,7,8,9,11,12,14,15,16-decahydro-1H-cyclopenta[a]phenanthren-3-one | 50-23-7 | 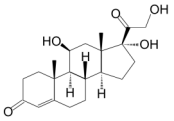 | 213-221 |

[a]Provided by Sigma-Aldrich.

reliability.[7] The positive environmental impact coupled with a higher kinetic performance of SFC represents nowadays a promising new strategy in pharmaceutical analysis.[7]

Accurate design and optimization of any pharmaceutical process or analytical technique that employs $scCO_2$ require that the solubility of the drug of interest in the supercritical solvent at different temperatures and pressures is available.[8,9] Since $CO_2$ is a linear molecule with no net dipole moment, it is able to dissolve non-polar compounds while its solvent power toward polar or ionic species is very limited. This last point, however, can be exploited by employing $scCO_2$ as an antisolvent in those micronization techniques (GAS, SAS, etc.) where its addition to an organic solution of the drug results in the precipitation of the active ingredient in controlled size or morphology.[5] On the other hand, also the RESS and SSI techniques can still be used because the limited solubility of polar drugs in pure $scCO_2$ can be overcome by simply adding a polar cosolvent (or modifier) to enhance it. As far as SFC is concerned elution of polar compounds can also be efficiently achieved by adding polar organic cosolvents with hydrogen-bond donor capacity, where alcohols generally represent the preferred choice.[7]

Ethanol and ethyl acetate are good examples of commonly used cosolvents, which can be employed in pharmaceutical processes since they are considered of lowest risk to human health (Class 3 of US Pharmacopeia).[4] Furthermore, it must be stressed that their use in any supercritical process does not compromise the above-cited advantage of obtaining a solvent-free pharmaceutical product since a simple flushing step with pure carbon dioxide may allow organic solvent residues to be extracted.[4,10]

Cortisone (COR) and hydrocortisone (HC) are poorly water-soluble corticosteroids that are among the most widely used drugs to treat many inflammatory and immune diseases.[11] Their molecular structures only differ for the presence of a carbonyl group or a hydroxy group on the 11th carbon of the cyclopenta [a] phenanthrene structure for COR and HC, respectively (Table 1). In particular, HC has already been used in the literature to obtain micro- and nanoparticles of the drug[12,13] or its incorporation into polymeric carriers[14,15] by means of micronization techniques where $scCO_2$ acts as an antisolvent. Furthermore, both drugs were tested in analytical techniques that make use of supercritical fluids.[16−18] For example, Kurečková and coworkers[16] employed organic-cosolvent-modified $scCO_2$ to extract steroids from biological samples as a preparation technique that preceded a high-performance liquid chromatography analysis. On the other hand, COR and HC were also selected as test compounds to investigate the retention of pharmaceutical compounds in different SFC techniques, where $scCO_2$ was modified by the addition of small percentages of ethanol or methanol.[17,18]

It is clear from the above discussion that the knowledge of solubility data of COR and HC in mixtures of organic solvents and $scCO_2$ may be of interest both to the applications where the $CO_2$ acts as a solvent (RESS, SSI, and SFC), since the addition of a cosolvent would enhance the drug solubility, and to those where the $CO_2$ is employed as an antisolvent (GAS, SAS, etc.), since the conditions to achieve antisolvent drug precipitation from an organic solution should be known.[1,4]

In this work, the solubility of COR and HC has been measured, for the first time, in a mixture of $scCO_2$ and 2, 3, or 4 mol % of cosolvent ethanol, at 318.15, 328.15, 348.15, and 373.15 K, and in the pressure range of 13−27 MPa. Under these working conditions, the $CO_2$−ethanol system displays a single homogeneous supercritical phase.[19−21] Preliminary experiments pointed out that without the addition of the



https://doi.org/10.1021/acs.jced.2c00690
J. Chem. Eng. Data 2023, 68, 601−611

cosolvent the solubility of both drugs in $scCO_2$ was too low and could be hardly detected or determined with acceptable accuracy. Tests were conducted in a semi-flow laboratory apparatus[22] and the solubility data were fitted with the most popular empirical and semi-empirical correlations reported in the literature for ternary systems.[23−32] The Garlapati−Madras (version with six parameters)[28] and the Reddy−Madras (version with seven parameters)[30] models resulted to be those with the highest correlation performance. Furthermore, the self-consistency of the experimental data was checked through the Méndez-Santiago−Teja test,[23] which is generally conducted with binary data[33] but has also been extended to the ternary solubility points measured in this work.

## 2. EXPERIMENTAL SECTION

**2.1. Materials.** IUPAC names, CAS number, structures, and melting ranges of COR and HC are reported in Table 1 while Table 2 lists the characteristics of the materials employed in this work.

**Table 2. List of Compounds Employed in This Work**

| chemical name | source | initial mole fraction purity | purification method |
|---|---|---|---|
| carbon dioxide | Siad S.p.A. (Italy) | 0.99998 | none |
| COR[a] | Sigma-Aldrich | ≥0.98 | none |
| HC[b] | Sigma-Aldrich | ≥0.98 | none |
| ethanol | Sigma-Aldrich | ≥0.998 | none |

[a]Cortisone. [b]Hydrocortisone.

**2.2. Apparatus and Analysis.** The solubility of COR and HC was measured with the experimental semi-flow apparatus reported in Figure 1. With respect to a previous version of the same apparatus,[22,34] this allows the drug solubility in ethanol-$scCO_2$ mixtures at different compositions to be measured.

The supercritical $CO_2$−ethanol mixture at the desired composition (2−4 mol % of ethanol) and pressure (13−27 MPa) is delivered, at a constant flow rate, to a saturation vessel by means of two syringe pumps, which are equipped with pressure indicators ($P$) and volumetric flow (VF) meters. Temperature indicators ($T$) are also set at the outlet of the syringe pumps. A micro-static mixing tee efficiently combines the $CO_2$, and the ethanol flows into a single stream, which is then heated at the working temperature (318.15−373.15 K) through a heat exchanger before feeding the saturation vessel. Both the heat exchanger and the saturation vessel are positioned inside a heating oven, which guarantees the constancy of temperature during each experimental test. The saturation vessel (diameter = 14 mm, length = 33 cm) contains a fixed bed of glass spheres where an excess amount of the solute (1 g) is finely dispersed. After achieving the saturation of the solute, the supercritical mixture is depressurized by means of a back-pressure regulator in an ethanol solvent trap where the previously solubilized drug is precipitated and collected. The back-pressure regulator also provides that the supercritical solvent flows at constant pressure through the vessel. A Coriolis-type mass flow (MF) meter, which is also coupled with a temperature sensor, is set before the entrance of the saturation vessel and allows both the flow rate and the density of the supercritical mixture to be measured. This last datum provides the experimental density of the binary supercritical solvent at the different working conditions of temperature, pressure, and ethanol mole fraction, to be used in data regression. The apparatus is also equipped with an additional ethanol flushing line (2 $mL \cdot min^{-1}$), which provides a continuous dilution of the saturated supercritical mixture just before the back-pressure regulator valve. This device prevents the valve to be clogged by the precipitated solute and guarantees its complete recovery, which avoids the solubility data to be underestimated. The flow rate of the ethanol

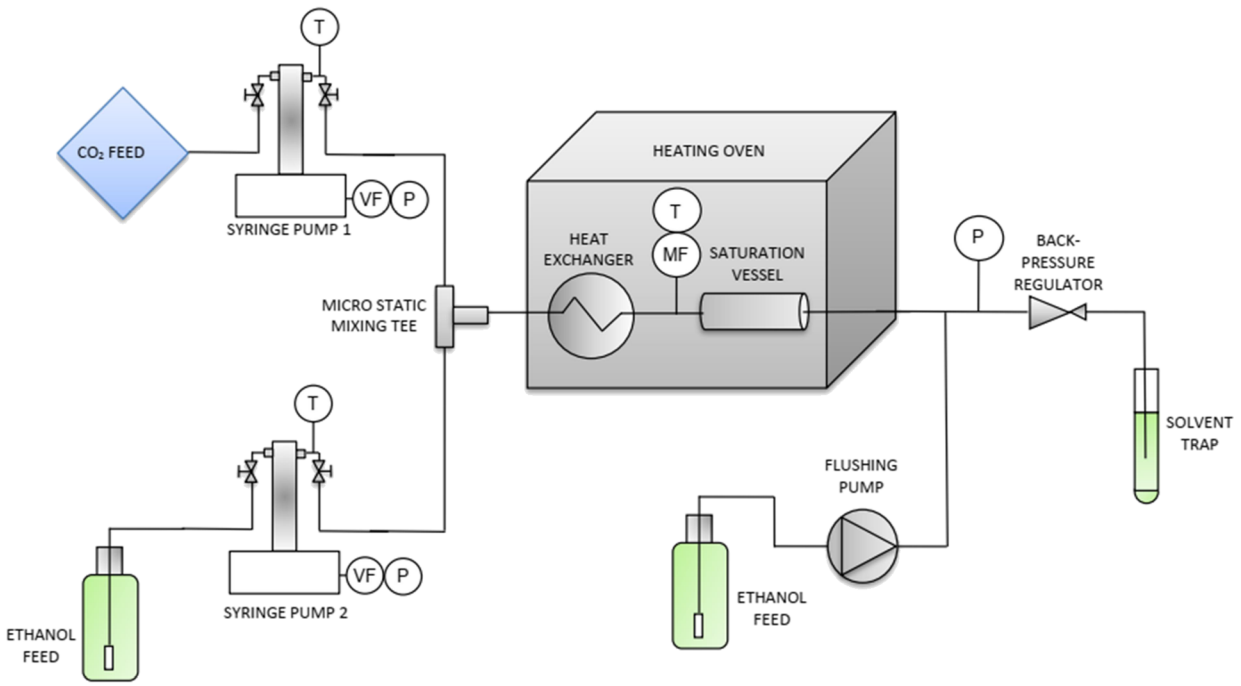


**Figure 1.** Scheme of the experimental apparatus employed for the solubility tests (VF, volumetric flow meter; MF, mass flow meter; and $T$ and $P$, temperature and pressure indicators).



https://doi.org/10.1021/acs.jced.2c00690
J. Chem. Eng. Data 2023, 68, 601−611

flushing line was accurately selected to avoid pressure fluctuations higher than ±0.1 MPa of the signal from the back-pressure regulator at all the investigated working conditions. Further details as well as the definition of the accuracy of this technique through the comparison with previous literature data are reported in previous studies.[22,34]

The solubility tests were conducted according to the following procedure that was repeated in triplicate at each experimental condition. The flow rates of the syringe pumps were selected to obtain a molar content of ethanol in the supercritical mixture, $y_3$, equal to 2, 3, or 4 mol %, and an overall flow rate of 0.6 g·min$^{-1}$. Preliminary tests at different contact times pointed out that the overall flow rate of the solvent mixture should be set at 0.6 g·min$^{-1}$ and that a transient period of 30 min should elapse to guarantee that saturation of the supercritical mixture had been reached.[22,34] The overall flow rate was monitored through the MF meter set inside the heating oven. After the 30-min transient period had elapsed, the solvent trap was filled in with a fresh amount of ethanol (10 g), which collected the drug dissolved by the supercritical mixture and the flushing solvent for 10 min. After sampling, an analytical balance allowed the final amount of the solution in the trap, $m_{sol}$ (g), to be determined while a UV spectrophotometer (maximum wavelengths for COR and HC equal to 238 and 242 nm, respectively) provided the drug mass fraction, $w_{drug}$, in the solution. The drug solubility, $y_2$, expressed as mole fraction, was calculated as follows:

$$y_2 = \frac{\frac{w_{drug} \times m_{sol}}{M_{drug}}}{\frac{w_{drug} \times m_{sol}}{M_{drug}} + \frac{m_{CO_2}}{M_{CO_2}} + \frac{m_{EtOH}}{M_{EtOH}}} \quad (1)$$

where $M_{drug}$, $M_{CO_2}$, and $M_{EtOH}$ are the molecular weights of the drug (COR or HC), $CO_2$, and ethanol, respectively, while $m_{CO_2}$ (g) and $m_{EtOH}$ (g) are the mass of $CO_2$ and ethanol that had been flowing through the vessel during the sampling time and had dissolved the recovered drug, respectively. The values of $m_{CO_2}$ and $m_{EtOH}$ were calculated based on the amounts pumped by the two syringe pumps, as follows:

$$m_{CO_2} = \dot{V}_{PUMP1} \times t \times \rho_{CO_2} \quad (2)$$

$$m_{EtOH} = \dot{V}_{PUMP2} \times t \times \rho_{EtOH} \quad (3)$$

where $\dot{V}_{PUMP1}$ (mL·min$^{-1}$) and $\dot{V}_{PUMP2}$ (mL·min$^{-1}$) are the pumped volumetric flow rates of $CO_2$ and ethanol, respectively, $t$ (=10 min) is the sampling time while $\rho_{CO_2}$ (g·mL$^{-1}$) and $\rho_{EtOH}$ (g·mL$^{-1}$) are the densities of the two solvents at the outlet section of each syringe pumps. $\rho_{CO_2}$ and $\rho_{EtOH}$ were calculated from the knowledge of the temperature and pressure at the outlet of each pump, which were provided by specific temperature ($T$) and pressure ($P$) indicators, and by means of Span–Wagner[35] and Dillon–Penoncello[36] equation of state, respectively. As far as the density of the supercritical $CO_2$–ethanol mixture at the working conditions set inside the saturation vessel is concerned, this was experimentally measured by the MF meter, as it has already been reported.

## 3. CORRELATION OF SOLUBILITY DATA

Density-based models are the simplest approach to correlate the experimental solubility data of solids in $scCO_2$. They are equations where the mole fraction solubility of the solid solute ($y_2$) is correlated with the density of the supercritical solvent ($\rho$) by means of different mathematical relationships, which may also include the equilibrium temperature ($T$) and pressure ($P$). When $scCO_2$ is mixed with a cosolvent, these correlations also include the dependence on the cosolvent mole fraction ($y_3$) in the mixture. Density-based models are quite popular in chemical engineering since, with respect to other solubility models, such as the equation-of-state (EOS) approach, they do not require the knowledge of any physical properties of the solute, such as the critical properties, acentric factor, sublimation pressure, etc. This is a significant advantage since these properties are not always easily determinable with high accuracy, which may negatively affect the correlation performance of the EOS models.[37]

As far as solute–cosolvent–$CO_2$ ternary mixtures are concerned, the first semi-empirical correlation was proposed by Mendez-Santiago and Teja in 2000.[23] Starting from the theory of dilute solutions and the definition of the effective Henry's constant Mendez-Santiago and Teja[23] assumed a linear dependence of the logarithm of the enhancement factor ($y_2P/P_{sub}$) on the solvent density and the cosolvent mole fraction, where $P_{sub}$ is the sublimation pressure of the solute. This correlation was subsequently modified by Sauceau and coworkers,[24] who incorporated a Clausius–Clapeyron-type dependence of $P_{sub}$ on temperature and a reference pressure ($P_{ref}$), leading to the equation form that is currently employed in the literature. Furthermore, it must be pointed out that the Mendez-Santiago–Teja approach also allows the self-consistency of the experimental data to be checked.[23,33]

A different semi-empirical approach is that proposed by solvate complex models, which assume that a solvate complex between the solute, the solvent, and, when present, the cosolvent molecules is formed at equilibrium. The well-known solvate complex model proposed by Chrastil[38] for binary systems in 1982 is generally considered the first pioneering example of this class of correlations. As far as ternary systems are concerned, the solvate complex models available in the literature are those reported by Gonzalez and coworkers,[25] Garlapati and Madras[27] as well as Reddy and Madras, who proposed both a five-[29] and a seven-parameter version.[30]

Eventually, a third correlation approach is that based on the empirical observation of the experimental trend of the solubility data versus temperature, pressure, solvent density, and cosolvent content as well as the review of the mathematical relationship of previously published models. The model proposed by Jouyban and coworkers[26] belongs to this correlation group as well as those proposed by Soltani and Mazloumi[31] and Sodeifian and Sajadian.[32] In addition, Garlapati and Madras[28] developed a six-parameter correlation following this approach as an alternative to the previously cited solvate complex model.[27]

Among all the different tested equations, the Reddy–Madras (version with seven parameters)[30] and the Garlapati–Madras models (version with six parameters)[28] resulted in the best correlation performances for COR and HC, respectively. The model proposed by Reddy and Madras in 2011[30] is a solvate complex model with seven regression parameters, where $\ln y_2$ displays a linear dependence on both $\rho$ and $\rho/T$:



https://doi.org/10.1021/acs.jced.2c00690
J. Chem. Eng. Data 2023, 68, 601–611

Table 3. Experimental and Calculated Mole Fraction Solubilities ($y_2$) of Cortisone in Ethanol/Supercritical $CO_2$ Mixtures at Different Compositions ($y_3$ Is the Mole Fraction of Ethanol, and $\rho$ Is the Experimental Density of the Ethanol/Supercritical $CO_2$ Mixture), Temperature $T$, and Pressure $P$[a]

| | | | | $y_2 \times 10^7$ | |
|---|---|---|---|---|---|
| $T$ (K) | $P$ (MPa) | $y_3$ | $\rho$ (kg·m$^{-3}$) | exptl | calcd[b] |
| 318.15 | 13.0 | 0.0210 | 702.7 | 5.8 | 6.4 |
| 318.15 | 15.0 | 0.0209 | 744.2 | 7.2 | 8.9 |
| 318.15 | 19.0 | 0.0207 | 799.3 | 10.2 | 13.2 |
| 318.15 | 23.0 | 0.0207 | 837.8 | 16.5 | 17.0 |
| 318.15 | 27.0 | 0.0206 | 867.2 | 17.9 | 20.5 |
| 328.15 | 13.0 | 0.0210 | 596.1 | 3.8 | 3.6 |
| 328.15 | 15.0 | 0.0209 | 663.5 | 6.7 | 6.4 |
| 328.15 | 19.0 | 0.0207 | 741.0 | 9.5 | 11.6 |
| 328.15 | 23.0 | 0.0207 | 789.5 | 17.4 | 16.4 |
| 328.15 | 27.0 | 0.0206 | 825.5 | 19.0 | 20.8 |
| 348.15 | 13.0 | 0.0210 | 377.5 | 1.4 | 1.3 |
| 348.15 | 15.0 | 0.0209 | 477.5 | 2.7 | 3.0 |
| 348.15 | 19.0 | 0.0207 | 609.7 | 8.4 | 8.5 |
| 348.15 | 23.0 | 0.0207 | 685.1 | 18.0 | 14.9 |
| 348.15 | 27.0 | 0.0206 | 735.7 | 24.3 | 21.0 |
| 373.15 | 13.0 | 0.0210 | 266.1 | 1.9 | 2.0 |
| 373.15 | 15.0 | 0.0209 | 330.2 | 3.0 | 3.1 |
| 373.15 | 19.0 | 0.0207 | 456.8 | 8.0 | 7.4 |
| 373.15 | 23.0 | 0.0206 | 551.9 | 14.4 | 14.2 |
| 373.15 | 27.0 | 0.0206 | 621.8 | 24.1 | 22.5 |
| 318.15 | 13.0 | 0.0315 | 714.1 | 16.2 | 14.8 |
| 318.15 | 15.0 | 0.0313 | 753.6 | 19.9 | 20.0 |
| 318.15 | 19.0 | 0.0311 | 804.7 | 26.9 | 28.4 |
| 318.15 | 23.0 | 0.0310 | 840.4 | 39.5 | 35.5 |
| 318.15 | 27.0 | 0.0309 | 869.5 | 43.5 | 42.4 |
| 328.15 | 13.0 | 0.0314 | 616.5 | 9.7 | 8.8 |
| 328.15 | 15.0 | 0.0313 | 677.5 | 14.2 | 14.6 |
| 328.15 | 19.0 | 0.0311 | 747.6 | 22.5 | 24.7 |
| 328.15 | 23.0 | 0.0310 | 794.1 | 33.4 | 33.9 |
| 328.15 | 27.0 | 0.0309 | 828.1 | 41.8 | 42.1 |
| 348.15 | 15.0 | 0.0313 | 488.9 | 5.9 | 6.3 |
| 348.15 | 19.0 | 0.0311 | 619.3 | 18.3 | 17.6 |
| 348.15 | 23.0 | 0.0310 | 690.0 | 29.9 | 29.3 |
| 348.15 | 27.0 | 0.0309 | 739.2 | 42.8 | 40.7 |
| 373.15 | 13.0 | 0.0315 | 270.4 | 3.8 | 3.8 |
| 373.15 | 15.0 | 0.0313 | 337.1 | 6.3 | 5.9 |
| 373.15 | 19.0 | 0.0311 | 462.6 | 12.9 | 14.0 |
| 373.15 | 23.0 | 0.0310 | 561.0 | 32.2 | 27.4 |
| 373.15 | 27.0 | 0.0309 | 626.4 | 46.6 | 41.7 |
| 318.15 | 13.0 | 0.0400 | 721.3 | 34.0 | 29.9 |
| 318.15 | 15.0 | 0.0399 | 758.2 | 38.9 | 39.5 |
| 318.15 | 19.0 | 0.0399 | 807.6 | 57.2 | 55.6 |
| 318.15 | 23.0 | 0.0400 | 841.7 | 77.2 | 69.2 |
| 318.15 | 27.0 | 0.0400 | 869.4 | 87.8 | 82.0 |
| 328.15 | 13.0 | 0.0400 | 618.3 | 17.7 | 16.4 |
| 328.15 | 15.0 | 0.0399 | 681.2 | 26.1 | 27.9 |
| 328.15 | 19.0 | 0.0400 | 750.8 | 44.0 | 47.8 |
| 328.15 | 23.0 | 0.0401 | 796.1 | 62.2 | 65.7 |
| 328.15 | 27.0 | 0.0400 | 828.7 | 84.4 | 80.3 |
| 348.15 | 13.0 | 0.0400 | 400.3 | 5.3 | 5.4 |
| 348.15 | 15.0 | 0.0402 | 501.9 | 12.5 | 12.7 |
| 348.15 | 19.0 | 0.0400 | 625.9 | 28.6 | 33.7 |
| 348.15 | 23.0 | 0.0401 | 695.2 | 52.5 | 56.0 |
| 348.15 | 27.0 | 0.0401 | 741.8 | 75.0 | 76.4 |
| 373.15 | 23.0 | 0.0399 | 565.5 | 41.4 | 48.7 |
| 373.15 | 27.0 | 0.0399 | 632.6 | 71.7 | 75.9 |

[a]Standard uncertainties for the temperature, pressure, ethanol mole fraction, density of the mixture, and solubility are $u(T) = 0.1$ K, $u(P) = 0.1$ MPa, $u(y_3) = 1 \times 10^{-4}$, $u(\rho) = 0.1$ kg/m$^3$, and $u(y_2) = 1 \times 10^{-8}$, respectively. [b]Reddy−Madras with seven parameters (2011).[30]

$$\ln y_2 = (k + \gamma - 1)\ln\left(\frac{P}{P_{ref}}\right) + \gamma \ln y_3 + \alpha_0 + \alpha_1\rho + \frac{\alpha_2 + \alpha_3\rho + \alpha_4 y_3}{T} \quad (4)$$

On the other hand, the Garlapati−Madras model (version with six parameters)[28] belongs to the last group of empirical correlations.[25,29,31,32] In the Garlapati−Madras model discussed here,[28] the $\ln y_2$ is a linear function of both $\rho$ and $\ln\rho$:

$$\ln y_2 = \alpha_0 + \alpha_1\rho + \frac{\alpha_2}{T} + \alpha_3 \ln\rho + \alpha_4 \ln y_3 + \alpha_5 \ln T \quad (5)$$

The experimental solubility data versus the experimental solvent density of the ethanol/supercritical $CO_2$ mixture were fitted with all the above-cited density-based models.[23−32] The models were fitted to the experimental data through nonlinear regression by minimizing the average absolute relative deviation between the calculated and experimental values. In Section 4.2, the correlation results obtained for COR and HC with the Reddy−Madras (version with seven parameters)[30] and the Garlapati−Madras models (version with six parameters)[28] are presented. Tables S1 and S2 of the Supporting Information report the complete list of the model equations as well as the values of the obtained regression parameters and the adjusted absolute average percent deviations (AARDs) between experimental and calculated solubility of the two drugs.

## 4. RESULTS AND DISCUSSION

**4.1. Experimental Results.** Both experimental and calculated mole fraction solubility values ($y_2$) of COR and HC in a mixture of $scCO_2$ and 2, 3, or 4 mol % of ethanol, at 318.15, 328.15, 348.15, and 373.15 K and in the pressure range of 13−27 MPa are reported in Tables 3 and 4, respectively. The calculated solubilities were obtained through the empirical models that exhibited the best correlation performance among those here discussed (Section 4.2). The density value ($\rho$) of the ethanol/supercritical $CO_2$ mixture was experimentally measured at different temperatures, pressures, and cosolvent content (Section 2).

The solubility of both drugs versus temperature, pressure, and the density of the solvent mixture displays the typical trend of a solute dissolved in $scCO_2$. At constant temperature, the solubility of the drug always increases when pressure increases since the density and, consequently, the solvating power of the fluid are increased. Instead, a temperature increase at constant pressure exhibits two competitive effects:[34,39,40] from one hand it positively affects the vapor pressure of the solute, resulting in a solubility enhancement, from the other it reduces the solvent



https://doi.org/10.1021/acs.jced.2c00690
J. Chem. Eng. Data 2023, 68, 601−611

Table 4. Experimental and Calculated Mole Fraction Solubilities ($y_2$) of Hydrocortisone in Ethanol/Supercritical $CO_2$ Mixtures at Different Compositions ($y_3$ Is the Mole Fraction of Ethanol, and $\rho$ Is the Experimental Density of the Ethanol/Supercritical $CO_2$ Mixture), Temperature $T$, and Pressure $P$[a]

| | | | | $y_2 \times 10^7$ | |
|---|---|---|---|---|---|
| $T$ (K) | $P$ (MPa) | $y_3$ | $\rho$ (kg·m$^{-3}$) | exptl | calcd[b] |
| 318.15 | 13.0 | 0.0199 | 702.2 | 1.3 | 2.0 |
| 318.15 | 15.0 | 0.0199 | 744.5 | 2.0 | 2.7 |
| 318.15 | 19.0 | 0.0200 | 799.7 | 3.2 | 3.9 |
| 318.15 | 23.0 | 0.0200 | 837.7 | 3.9 | 5.1 |
| 318.15 | 27.0 | 0.0200 | 867.4 | 4.8 | 6.2 |
| 328.15 | 13.0 | 0.0200 | 588.7 | 1.0 | 1.1 |
| 328.15 | 15.0 | 0.0200 | 662.4 | 1.5 | 2.0 |
| 328.15 | 19.0 | 0.0199 | 740.3 | 3.1 | 3.5 |
| 328.15 | 23.0 | 0.0200 | 788.4 | 5.9 | 4.9 |
| 328.15 | 27.0 | 0.0200 | 824.4 | 6.1 | 6.3 |
| 348.15 | 15.0 | 0.0199 | 471.9 | 0.7 | 0.7 |
| 348.15 | 19.0 | 0.0199 | 608.2 | 2.1 | 2.6 |
| 348.15 | 23.0 | 0.0200 | 684.4 | 5.0 | 4.7 |
| 348.15 | 27.0 | 0.0200 | 734.8 | 7.3 | 6.8 |
| 373.15 | 19.0 | 0.0200 | 453.8 | 2.0 | 1.7 |
| 373.15 | 23.0 | 0.0199 | 551.7 | 5.4 | 4.4 |
| 318.15 | 13.0 | 0.0316 | 715.2 | 6.9 | 5.1 |
| 318.15 | 15.0 | 0.0316 | 753.6 | 7.2 | 6.7 |
| 318.15 | 19.0 | 0.0313 | 804.7 | 9.9 | 9.4 |
| 318.15 | 23.0 | 0.0311 | 841.3 | 10.7 | 11.9 |
| 318.15 | 27.0 | 0.0310 | 869.1 | 13.1 | 14.2 |
| 328.15 | 13.0 | 0.0319 | 614.4 | 3.8 | 3.2 |
| 328.15 | 15.0 | 0.0317 | 676.7 | 5.4 | 5.2 |
| 328.15 | 19.0 | 0.0314 | 748.1 | 8.5 | 8.6 |
| 328.15 | 23.0 | 0.0312 | 793.6 | 12.2 | 11.7 |
| 328.15 | 27.0 | 0.0311 | 827.6 | 15.3 | 14.7 |
| 348.15 | 13.0 | 0.0317 | 390.2 | 0.8 | 0.7 |
| 348.15 | 15.0 | 0.0315 | 493.1 | 2.0 | 2.1 |
| 348.15 | 19.0 | 0.0313 | 620.4 | 6.6 | 6.5 |
| 348.15 | 23.0 | 0.0311 | 691.8 | 10.8 | 11.3 |
| 348.15 | 27.0 | 0.0311 | 740.3 | 16.2 | 16.2 |
| 373.15 | 13.0 | 0.0397 | 266.5 | 0.6 | 0.6 |
| 373.15 | 15.0 | 0.0396 | 333.2 | 1.2 | 1.5 |
| 373.15 | 23.0 | 0.0310 | 561.5 | 12.3 | 11.0 |
| 373.15 | 27.0 | 0.0310 | 627.1 | 22.0 | 19.1 |
| 318.15 | 13.0 | 0.0401 | 721.4 | 10.0 | 8.3 |
| 318.15 | 15.0 | 0.0401 | 757.5 | 12.0 | 10.8 |
| 318.15 | 19.0 | 0.0400 | 806.4 | 16.6 | 15.1 |
| 318.15 | 23.0 | 0.0400 | 841.9 | 17.7 | 19.2 |
| 318.15 | 27.0 | 0.0400 | 869.8 | 25.5 | 22.9 |
| 328.15 | 13.0 | 0.0401 | 621.6 | 5.0 | 5.2 |
| 328.15 | 15.0 | 0.0399 | 683.4 | 7.3 | 8.4 |
| 328.15 | 19.0 | 0.0399 | 751.7 | 12.5 | 13.9 |
| 328.15 | 23.0 | 0.0399 | 795.9 | 19.0 | 18.9 |
| 328.15 | 27.0 | 0.0400 | 828.7 | 24.8 | 23.7 |
| 348.15 | 13.0 | 0.0401 | 399.4 | 1.3 | 1.2 |
| 348.15 | 15.0 | 0.0401 | 503.2 | 3.8 | 3.7 |
| 348.15 | 19.0 | 0.0399 | 625.5 | 9.7 | 10.8 |
| 348.15 | 23.0 | 0.0401 | 696.4 | 18.2 | 18.8 |
| 348.15 | 27.0 | 0.0400 | 742.8 | 25.9 | 26.5 |
| 373.15 | 13.0 | 0.0402 | 276.1 | 0.7 | 0.7 |
| 373.15 | 15.0 | 0.0400 | 341.1 | 1.7 | 1.7 |
| 373.15 | 19.0 | 0.0401 | 472.3 | 6.7 | 7.7 |
| 373.15 | 23.0 | 0.0401 | 565.2 | 15.9 | 18.4 |
| 373.15 | 27.0 | 0.0400 | 631.2 | 29.4 | 31.9 |

[a]Standard uncertainties for the temperature, pressure, ethanol mole fraction, density of the mixture, and solubility are $u(T) = 0.1$ K, $u(P) = 0.1$ MPa, $u(y_3) = 1 \times 10^{-4}$, $u(\rho) = 0.1$ kg/m$^3$, and $u(y_2) = 1 \times 10^{-8}$, respectively. [b]Garlapati−Madras with six parameters (2010).[28]

density, which involves a reduction in the drug solubility. For this reason, it is common practice to plot the solubility isotherms versus the solvent density instead of pressure. In this way, only the positive effect of temperature over the solute solubility is displayed while its negative effect versus the solvent density is included in the independent variable of the plot. Figure 2 shows, as an example, the solubility trend versus temperature and solvent density of COR with a 3 mol % content of cosolvent ethanol in the mixture.

As it has already been mentioned, preliminary experiments conducted without the addition of ethanol pointed out that the solubility of both drugs in $scCO_2$ was too low to be determined with acceptable accuracy. The addition of ethanol is beneficial to both drugs and the higher the ethanol content the higher the drug solubility in the supercritical mixture. Figure 3 shows, for example, the effect of the cosolvent mole fraction on the solubility trend versus pressure for HC at constant temperature (348.15 K). Similar trends were observed for both drugs at different temperatures. Depending on the drug and the working conditions, a three to five times solubility enhancement was observed for both drugs when the ethanol content was doubled from 2 to 4 mol %.

The increase in solute solubility caused by the addition of small amounts of cosolvent to $scCO_2$ was explained in the literature[41] by supposing that the local cosolvent concentration surrounding the solute molecules is higher than the bulk one due to the high affinity between the solute and the cosolvent, which results in stronger molecular interactions between the involved chemical species. According to Zhang and coworkers,[42] the addition of a cosolvent affects the enthalpy and the entropy changes of the dissolution process in opposite ways: while the first one is decreased (i.e., the dissolution process becomes less exothermic), the second is strongly increased. Since the entropy effect is dominant, the addition of the cosolvent results in an overall decrease of the Gibbs free energy variation, which favors an increase of the solute solubility.

A comparison between the data reported in Tables 3 and 4 points out that COR is more soluble in the ethanol-$scCO_2$ mixture than HC. On average solubility data of COR are 3.5 times higher than those of HC. Figure 4 reports an example of a comparison between the solubility trends versus the density of the supercritical solvent of COR and HC at a fixed temperature value (318.15 K) and different ethanol contents in the solvent mixture.

The solubility difference between the two drugs is quite significant even though their molecular structures are very similar (Table 1). This difference could be related to the different solubility in ethanol of the two drugs. According to the *ChemSpider* database,[43] COR solubility in ethanol is approximately six times higher than that of HC, despite the fact that COR only displays a carbonyl group instead of a hydroxy



https://doi.org/10.1021/acs.jced.2c00690
J. Chem. Eng. Data 2023, 68, 601−611

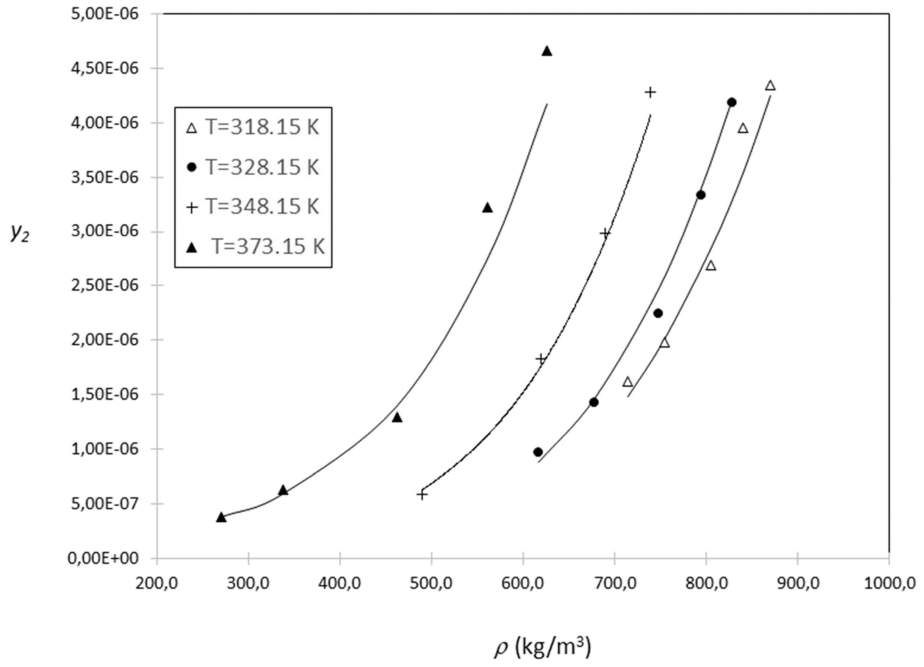


**Figure 2.** Typical trend of the experimental mole fraction solubility of the solute ($y_2$) versus temperature ($T$) and the experimental density ($\rho$) of the ethanol/supercritical $CO_2$ mixture (data in the plot refer to cortisone in an ethanol/supercritical $CO_2$ mixture with 3 mol % of ethanol)—the lines represent the solubility values calculated through Reddy–Madras correlation (version with seven parameters).[30]

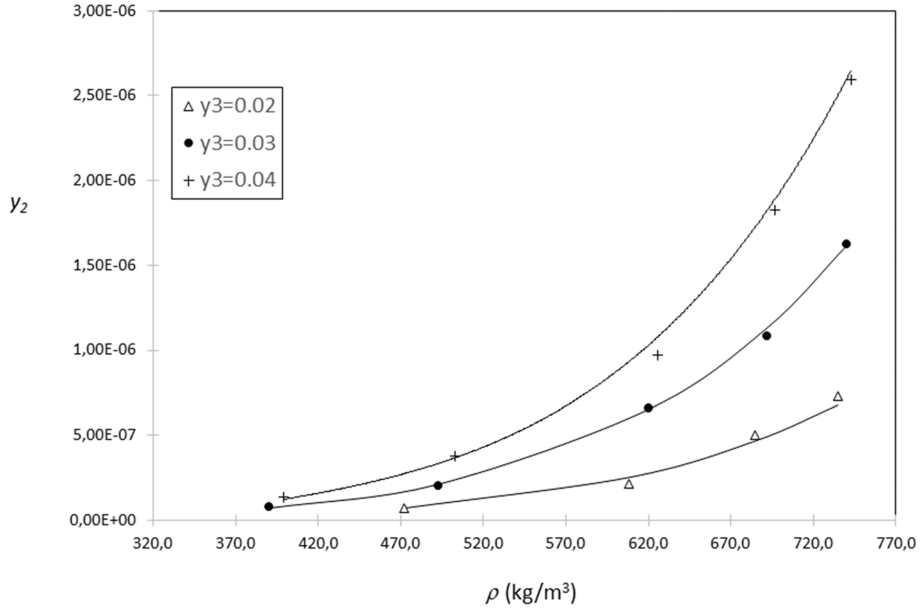


**Figure 3.** Typical effect of the ethanol mole fraction ($y_3$) in the ethanol/supercritical $CO_2$ mixture on the trend of the experimental mole fraction solubility of the solute ($y_2$) versus the experimental density ($\rho$) of the ethanol/supercritical $CO_2$ mixture (data in the plot refer to hydrocortisone at $T$ = 348.15 K)—the lines represent the solubility values calculated through the Garlapati–Madras correlation (version with six parameters).[28]

one on the 11th carbon of the cyclopenta[*a*]phenanthrene structure. This significant solubility difference in the pure alcohol is, then, maintained when this is mixed with the supercritical solvent.

**4.2. Data Correlation.** The experimental data of this work were correlated with all the models briefly described in Section 3. This section reports the results obtained for COR and HC with the best-correlating equations, while Tables S1 and S2 of the Supporting Information report the regression parameters and AARDs between experimental and calculated solubility of the two drugs for the complete list of models.

In Tables 3 and 4 the experimental solubility data are compared with those calculated with the best-correlating model for each drug, i.e., the Reddy–Madras (version with seven parameters)[30] for COR and the Garlapati–Madras models (version with six parameters)[28] for HC, respectively. Table 5 reports, for each drug, the regression parameters of the best-correlating models as well as the adjusted coefficient of determination ($R^2_{adj}$) and the AARD% between experimental and calculated solubility, which is defined as follows:



https://doi.org/10.1021/acs.jced.2c00690
J. Chem. Eng. Data 2023, 68, 601–611

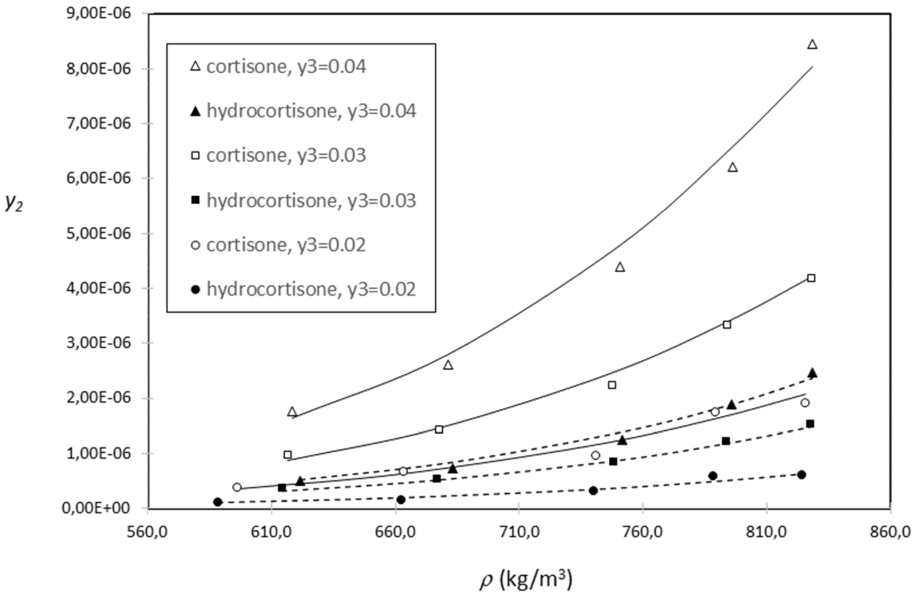


**Figure 4.** Example of comparison between the trends of the experimental mole fraction solubilities ($y_2$) of cortisone and hydrocortisone versus the experimental density ($\rho$) of the ethanol/supercritical $CO_2$ mixture at different values of the ethanol mole fraction ($y_3$) in the mixture (data in the plot refer to $T$ = 328.15 K)—the continuous and dotted lines represent the cortisone and hydrocortisone solubility values calculated through the Reddy–Madras (version with seven parameters)[30] and the Garlapati–Madras (version with six parameters)[28] correlations, respectively.

**Table 5. Regression Parameters, Coefficient of Determination ($R^2_{adj}$), and the Adjusted Absolute Average Percent Deviation (AARD%) of the Density-Based Models Used To Fit the Experimental Solubility of Cortisone (COR) and Hydrocortisone (HC)**

| drug | model | parameters | $R^2_{adj}$ | AARD% |
|---|---|---|---|---|
| COR | Reddy–Madras[a] | $k$ = 0.56099, $\gamma$ = − 0.40142, $\alpha_0$ = 9.6782, $\alpha_1$ = − 5.4589 × $10^{-3}$, $\alpha_2$ = − 9.8264 × $10^3$, $\alpha_3$ = 5.231, and $\alpha_4$ = 2.6756 × $10^4$ | 0.9859 | 8.8% |
| HC | Garlapati–Madras[b] | $\alpha_0$ = − 4.3562 × $10^2$, $\alpha_1$ = 2.1132 × $10^{-3}$, $\alpha_2$ = 1.6475 × $10^4$, $\alpha_3$ = 3.7648, $\alpha_4$ = 1.8683, and $\alpha_5$ = 60.659 | 0.9746 | 11.6% |

[a] $\ln y_2 = (k+\gamma-1)\ln\left(\frac{P}{P_{ref}}\right) + \gamma \ln y_3 + \alpha_0 + \alpha_1\rho + \frac{\alpha_2+\alpha_3\rho+\alpha_4 y_3}{T}$,

where $y_2$ is the solute mole fraction solubility, $y_3$ is the mole fraction of ethanol, $\rho$ (kg·m$^{-3}$) is the density of the supercritical $CO_2$/ethanol mixture, $T$ (K) is temperature, $P$ (MPa) is pressure, and $P_{ref}$ = 0.1 MPa. [b] $\ln y_2 = \alpha_0 + \alpha_1\rho + \frac{\alpha_2}{T} + \alpha_3 \ln\rho + \alpha_4 \ln y_3 + \alpha_5 \ln T$, where $y_2$ is the solute mole fraction solubility, $y_3$ is the mole fraction of ethanol, $\rho$ (kg·m$^{-3}$) is the density of the supercritical $CO_2$/ethanol mixture, $T$ (K) is temperature, and $P$ (MPa) is pressure.

$$\text{AARD\%} = \frac{100}{n-z}\sum_{i=1}^{n}\left|\frac{y_{2i}^{exp} - y_{2i}^{cal}}{y_{2i}^{exp}}\right| \quad (6)$$

where $n$ is the number of experimental points and $z$ is the number of parameters of the correlation.

Both models produced an accurate fit of the experimental data with $R^2_{adj}$ values almost approaching unity. However, some differences of the AARD% values can be observed. As far as COR is concerned, the Reddy–Madras model displays the lowest AARD% value (8.8%), while the Garlapati–Madras approach results in a higher deviation (11.6%) for HC. This trend is confirmed by all models (Tables S1 and S2): the regression of the HC experimental data generally results in higher deviations than COR. This is probably related to the fact that the solubility of HC is lower than the COR one and low drug concentrations in the supercritical mixture are more difficult to measure.

**4.3. Self-Consistency Test.** As it has been mentioned in Section 3, the Méndez-Santiago–Teja correlation also allows the self-consistency of experimental data to be checked. This test is generally conducted with binary data[33] and consists in rewriting the equation model so that when experimental data are "self-consistent" their plot according to the "rewritten model" results in all isotherms collapsing into a single line.

In the literature, the above-cited approach has also been extended to ternary systems. For this purpose, the Méndez-Santiago–Teja correlation can be more conveniently written in the following form:[23]

$$T\ln\left(\frac{P}{P_{ref}}y_2\right) - \alpha_2 T = \alpha_0 + \alpha_1\rho + \alpha_3 y_3 \quad (7)$$

In this case, the isotherms at fixed cosolvent concentrations ($y_3$) should collapse into a single line, and the self-consistency test is considered satisfactory if the experimental data at fixed $y_3$ collapse into parallel lines when they are plotted versus $\rho$ according to eq 5. However, if eq 6 is rearranged as follows:

$$T\ln\left(\frac{P}{P_{ref}}y_2\right) - \alpha_2 T - \alpha_3 y_3 = \alpha_0 + \alpha_1\rho \quad (8)$$

the plot of all experimental data at different temperatures, pressures, and $y_3$ values should collapse into a single line when they are plotted versus $\rho$ according to eq 6, as it occurs in the original self-consistency tests for binary systems.

The approach proposed in eq 6 has been adopted with the ternary solubility points measured in this work and is reported in Figures 5 and 6 for COR and HC, respectively. The figures point out that the experimental data of both drugs are satisfactorily consistent, with COR displaying better linearity. In fact, the plot for HC in Figure 6 shows that, even though all


https://doi.org/10.1021/acs.jced.2c00690
J. Chem. Eng. Data 2023, 68, 601−611

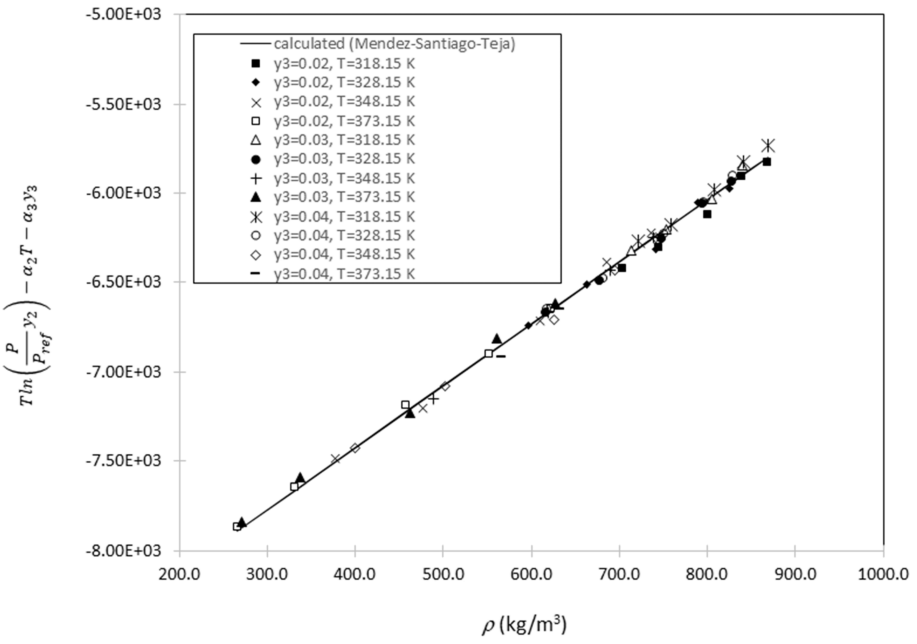


**Figure 5.** Méndez-Santiago−Teja self-consistency test for cortisone ($y_2$ is the mole fraction solubility of the solute, $y_3$ is the ethanol mole fraction in the ethanol/supercritical $CO_2$ mixture, $\rho$ is the experimental density of the ethanol/supercritical $CO_2$ mixture, $P$ is the pressure, $T$ is the temperature, and $\alpha_2$, $\alpha_3$ are parameters of the Méndez-Santiago Teja model[23] while $P_{ref}$ = 0.1 MPa).

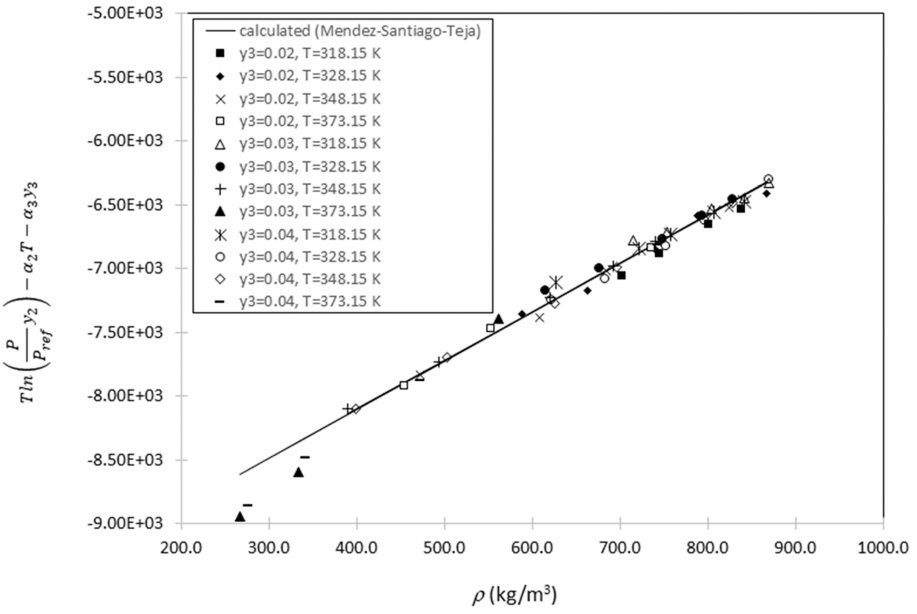


**Figure 6.** Méndez-Santiago−Teja self-consistency test for hydrocortisone ($y_2$ is the mole fraction solubility of the solute, $y_3$ is the ethanol mole fraction in the ethanol/supercritical $CO_2$ mixture, $\rho$ is the experimental density of the ethanol/supercritical $CO_2$ mixture, $P$ is the pressure, $T$ is the temperature, and $\alpha_2$, $\alpha_3$ are parameters of the Méndez-Santiago−Teja model,[23] while $P_{ref}$ = 0.1 MPa).

data collapse into a single curve, some low-density points do not follow the linear trend. This partial deviation is due to the fact that, according to the results reported in Section 4.2 the best correlation performance for HC has been obtained with a model displaying a linear dependence of $\ln y_2$ on both $\rho$ and $\ln\rho$ while the Méndez-Santiago−Teja approach is based on a dependence of $\ln y_2$ on $\rho$. On the other hand, the solubility data obtained for COR is better described by a correlation that follows a linear dependence of $\ln y_2$ on $\rho$, which gives reason for the better fit reported in Figure 5.

## 5. CONCLUSIONS

The solubility of COR and HC has been determined, for the first time, in a mixture of $scCO_2$ and 2, 3, or 4 mol % of cosolvent ethanol, at 318.15, 328.15, 348.15, and 373.15 K, and in the pressure range of 13−27 MPa. Despite the fact that the two drugs exhibit very similar molecular structures, the solubility of COR in the ethanol-$scCO_2$ mixture is in the range of $1.36 \times 10^{-7}$ to $9.13 \times 10^{-6}$ mole fraction while that of HC is in the range of $5.02 \times 10^{-8}$ to $2.94 \times 10^{-6}$ mole fraction. The higher solubility of COR is congruent with its higher solubility in pure ethanol, which is maintained when the alcohol is mixed


https://doi.org/10.1021/acs.jced.2c00690
J. Chem. Eng. Data 2023, 68, 601−611

with the supercritical solvent. The experimental solubility data were successfully correlated with the most popular empirical and semi-empirical density-based models for ternary systems. Among all the investigated equations, the two best-correlating ones are here reported. The Reddy−Madras model (version with seven regression parameters) proved to be the best one for COR with an AARD% of 8.8%, while the Garlapati−Madras model (version with six regression parameters) provided the best fitting for HC with an AARD% of 11.6%. The reliability of the experimental results was also confirmed by the positive response to the Méndez-Santiago−Teja self-consistency test, which is generally conducted with binary data and has been extended to the ternary solubility points measured in this work. It can, then, be concluded that the measured solubility data and the optimized fitting parameters of the models can be an effective tool if any pharmaceutical process or analytical technique involving the use of COR or HC in the presence of ethanol-scCO$_2$ mixtures is going to be designed.

## ■ ASSOCIATED CONTENT

### Supporting Information

The Supporting Information is available free of charge at https://pubs.acs.org/doi/10.1021/acs.jced.2c00690.

All the model equations, regression parameters, and adjusted absolute average percent deviations (AARD%) between the experimental and calculated solubility of the two drugs (PDF)

## ■ AUTHOR INFORMATION


### Corresponding Author

**Mauro Banchero** − *Dipartimento Scienza Applicata e Tecnologia, Politecnico di Torino, I-10129 Torino, Italy;* orcid.org/0000-0003-1508-3921; Phone: +39 011 0904703; Email: mauro.banchero@polito.it

### Author

**Luigi Manna** − *Dipartimento Scienza Applicata e Tecnologia, Politecnico di Torino, I-10129 Torino, Italy*

Complete contact information is available at: https://pubs.acs.org/10.1021/acs.jced.2c00690


### Notes

The authors declare no competing financial interest.

## ■ REFERENCES


(1) Kankala, R. K.; Zhang, Y. S.; Wang, S.-B.; Lee, C.-H.; Chen, A.-Z. Supercritical Fluid Technology: An Emphasis on Drug Delivery and Related Biomedical Applications. *Adv. Healthcare Mater.* **2017**, *6*, No. 1700433.

(2) Kumar, P.; Singh, C. A Study on Solubility Enhancement Methods for Poorly Water Soluble Drugs. *Am. J. Pharmacol. Sci.* **2013**, *1*, 67−73.

(3) Sun, J.; Wang, F.; Sui, Y.; She, Z.; Zhai, W.; Wang, C.; Deng, Y. Effect of particle size on solubility, dissolution rate, and oral bioavailability: Evaluation using coenzyme $Q_{10}$ as naked nanocrystals. *Int. J. Nanomed.* **2012**, *7*, 5733−5744.

(4) Gurikov, P.; Smirnova, I. Amorphization of Drugs by Adsorptive Precipitation from Supercritical Solutions: A Review. *J. Supercrit. Fluids* **2018**, *132*, 105−125.

(5) Nuchuchua, O.; Nejadnik, M. R.; Goulooze, S. C.; Lješković, N. J.; Every, H. A.; Jiskoot, W. Characterization of drug delivery particles produced by supercritical carbon dioxide technologies. *J. Supercrit. Fluids* **2017**, *128*, 244−262.

(6) Barros, A. A.; Silva, J. M.; Craveiro, R.; Paiva, A.; Reis, R. L.; Duarte, A. R. C. Green solvents for enhanced impregnation processes in biomedicine. *Curr. Opin. Green Sustainable Chem.* **2017**, *5*, 82−87.

(7) Desfontaine, V.; Guillarme, D.; Francotte, E.; Novakova, L. Supercritical fluid chromatography in pharmaceutical analysis. *J. Pharm. Biomed.* **2015**, *113*, 56−71.

(8) Knez, Z.; Cör, D.; Knez-Hrnčič, M. Solubility of solids in sub- and supercritical fluids: a review 2010-2017. *J. Chem. Eng. Data* **2018**, *63*, 860−884.

(9) Peper, S.; Fonseca, J. M. S.; Dohrn, R. High-pressure fluid-phase equilibria: Trends, recent developments, and systems investigated (2009−2012). *Fluid Phase Equilib.* **2019**, *484*, 126−224.

(10) Baldino, L.; Concilio, S.; Cardea, S.; De Marco, I.; Reverchon, E. Complete glutaraldehyde elimination during chitosan hydrogel drying by SC-$CO_2$ processing. *J. Supercrit. Fluids* **2015**, *103*, 70−76.

(11) Barnes, P. J. How corticosteroids control inflammation: Quintiles Prize Lecture 2005. *Br. J. Pharmacol.* **2006**, *148*, 245−254.

(12) Velaga, S. P.; Ghaderi, R.; Carlfors, J. Preparation and Characterisation of Hydrocortisone Particles Using a Supercritical Fluids Extraction Process. *Int. J. Pharm.* **2002**, *231*, 155−166.

(13) Thakur, R.; Gupta, R. B. Production of Hydrocortisone Micro- and Nano-particles Using Supercritical Anti-solvent with Enhanced Mass Transfer. *Chem. Eng. Commun.* **2006**, *193*, 293−305.

(14) Corrigan, O. I.; Crean, A. M. Comparative Physicochemical Properties of Hydrocortisone/PVP Composites Prepared Using Supercritical Carbon Dioxide by the GAS Anti-Solvent Recrystallization Process, by Coprecipitation and by Spray Drying. *Int. J. Pharm.* **2002**, *245*, 75−82.

(15) Wang, Y.; Wang, Y.; Yang, J.; Pfeffer, R.; Dave, R.; Michniak, B. The application of a supercritical antisolvent process for sustained drug delivery. *Powder Technol.* **2006**, *164*, 94−102.

(16) Kurečková, K.; Maralíková, B.; Ventura, K. Supercritical fluid extraction of steroids from biological samples and first experience with solid-phase microextraction−liquid chromatography. *J. Chromatogr. B: Anal. Technol. Biomed. Life Sci.* **2002**, *770*, 83−89.

(17) Berger, T. A. Characterization of a 2.6 $\mu$m Kinetex porous shell hydrophilic interaction liquid chromatography column in supercritical fluid chromatography with a comparison to 3 $\mu$m totally porous silica. *J. Chromatogr. A* **2011**, *1218*, 4559−4568.

(18) Andri, B.; Dispas, A.; Marini, R. D.; Hubert, P.; Sassiat, P.; Al Bakain, R.; Thiébaut, D.; Vial, J. Combination of partial least squares regression and design of experiments to model the retention of pharmaceutical compounds in supercritical fluid chromatography. *J. Chromatogr. A* **2017**, *1491*, 182−194.

(19) Sima, S.; Feroiu, V.; Geană, D. New High Pressure Vapor-Liquid Equilibrium and Density Predictions for the Carbon Dioxide + Ethanol System. *J. Chem. Eng. Data* **2011**, *56*, 5052−5059.

(20) Chatwell, R. S.; Guevara-Carrion, G.; Gaponenko, Y.; Shevtsova, V.; Vrabec, J. Diffusion of the carbon dioxide−ethanol mixture in the extended critical region. *Phys. Chem. Chem. Phys.* **2021**, *23*, 3106−3115.

(21) Mehl, A.; Nascimento, F. P.; Falcão, P. W.; Pessoa, F. L. P.; Cardozo-Filho, L.Vapor-Liquid Equilibrium of Carbon Dioxide + Ethanol: Experimental Measurements with Acoustic Method and Thermodynamic Modeling. *J Thermodyn.*, 20112011, 251075, DOI: 10.1155/2011/251075.

(22) Banchero, M.; Manna, L. Solubility of fenamate drugs in supercritical carbon dioxide by using a semi-flow apparatus with a continuous solvent-washing step in the depressurization line. *J. Supercrit. Fluids* **2016**, *107*, 400−407.

(23) Mendez-Santiago, J.; Teja, A. S. Solubility of Solids in Supercritical Fluids: Consistency of Data and a New Model for Cosolvent Systems. *Ind. Eng. Chem. Res.* **2000**, *39*, 4767−4771.

(24) Sauceau, M.; Letourneau, J. J.; Richon, D.; Fages, J. Enhanced density-based models for solid compound solubilities in supercritical carbon dioxide with cosolvents. *Fluid Phase Equilib.* **2003**, *208*, 99−113.

(25) Gonzalez, J. C.; Vieytes, M. R.; Botana, M. B.; Vieites, J. M.; Botana, L. M. Modified mass action law-based model to correlate the

solubility of solids and liquids in entrained supercritical carbon dioxide. *J. Chromatogr. A* **2001**, *910*, 119−125.
(26) Jouyban, A.; Khoubnasabjafari, M.; Chan, H. K. Modeling the Entrainer Effects on Solubility of Solutes in Supercritical Carbon Dioxide. *Chem. Pharm. Bull.* **2005**, *53*, 290−295.
(27) Garlapati, C.; Madras, G. Solubilities of solids in supercritical fluids using dimensionally consistent modified solvate complex models. *Fluid Phase Equilib.* **2009**, *283*, 97−101.
(28) Garlapati, C.; Madras, G. New empirical expressions to correlate solubilities of solids in supercritical carbon dioxide. *Thermochim. Acta* **2010**, *500*, 123−127.
(29) Reddy, S. N.; Madras, G. A new semi-empirical model for correlating the solubilities of solids in supercritical carbon dioxide with cosolvents. *Fluid Phase Equilib.* **2011**, *310*, 207−212.
(30) Reddy, S. N.; Madras, G. Modeling of ternary solubilities of solids in supercritical carbon dioxide in the presence of cosolvents or cosolutes. *J. Supercrit. Fluids* **2012**, *63*, 105−114.
(31) Soltani, S.; Mazloumi, S. H. A new empirical model to correlate solute solubility in supercritical carbon dioxide in presence of co-solvent. *Chem. Eng. Res. Des.* **2017**, *125*, 79−87.
(32) Sodeifian, G.; Sajadian, S. A. Experimental measurement of solubilities of sertraline hydrochloride in supercritical carbon dioxide with/without menthol: data correlation. *J. Supercrit. Fluids* **2019**, *149*, 79−87.
(33) Méndez-Santiago, J.; Teja, A. S. The solubility of solids in supercritical fluids. *Fluid Phase Equilib.* **1999**, *158−160*, 501−510.
(34) Manna, L.; Banchero, M. Solubility of Tolbutamide and Chlorpropamide in Supercritical Carbon Dioxide. *J. Chem. Eng. Data* **2018**, *63*, 1745−1751.
(35) Span, R.; Wagner, W. A new equation of state for carbon dioxide covering the fluid region from the triple-point temperature to 1100 K at pressures up to 800 MPa. *J. Phys. Chem. Ref. Data* **1996**, *25*, 1509−1596.
(36) Dillon, H. E.; Penoncello, S. G. A Fundamental Equation for Calculation of the Thermodynamic Properties of Ethanol. *Int. J. Thermophys.* **2004**, *25*, 321−335.
(37) Skerget, M.; Knez, Z.; Knez-Hrncik, M. Solubility of Solids in Sub- and Supercritical Fluids: a Review. *J. Chem. Eng. Data* **2011**, *56*, 694−719.
(38) Chrastil, J. Solubility of solids and liquids in supercritical gases. *J. Phys. Chem.* **1982**, *86*, 3016−3021.
(39) Lashkarbolooki, M.; Hezave, A. Z.; Rahnama, Y.; Ozlati, R.; Rajaei, H.; Esmaeilzadeh, F. Solubility of cyproheptadine in supercritical carbon dioxide; experimental and modeling approaches. *J. Supercrit. Fluids* **2013**, *84*, 13−19.
(40) Ndayishimiye, J.; Popat, A.; Kumeria, T.; Blaskovich, M. A. T.; Robert Falconer, J. Supercritical carbon dioxide assisted complexation of benznidazole: γ-cyclodextrin for improved dissolution. *Int. J. Pharm.* **2021**, *596*, No. 120240.
(41) Ellington, J. B.; Park, K. M.; Brennecke, J. F. Effect of local composition enhancements on the esterification of phthalic anhydride with methanol in supercritical carbon dioxide. *Ind. Eng. Chem. Res.* **1994**, *33*, 965−974.
(42) Zhang, X.; Han, B.; Hou, Z.; Zhang, J.; Liu, Z.; Jiang, T.; He, J.; Li, H. Why do co-solvents enhance the solubility of solutes in supercritical fluids? New evidence and opinion. *Chem. − Eur. J.* **2002**, *8*, 5107−5111.
(43) *ChemSpider Home Page*. http://www.chemspider.com/ (accessed December 12, 2022).





https://doi.org/10.1021/acs.jced.2c00690
*J. Chem. Eng. Data* 2023, 68, 601−611